Received: 10 February 2020 | Revised: 8 September 2020 | Accepted: 22 September 2020

DOI: 10.1111/ejn.14993

RESEARCH REPORT

EJN European Journal of Neuroscience FENS WILEY

Constraint-induced movement therapy promotes motor recovery after neonatal stroke in the absence of neural precursor activation

Kelsey V. Adams[1] | **Neemat Mahmud**[2] | **Madeline Green-Holland**[3] | **Ilan Vonderwalde**[4] | **Daisuke Umebayashi**[5] | **Nadia Sachewsky**[6,2] | **Brenda L. Coles**[5] | **Derek van der Kooy**[5,6,7] | **Cindi M. Morshead**[2,4,6,7,8]

[1]Institute of Medical Science, University of Toronto, Toronto, ON, Canada

[2]Department of Surgery, Division of Anatomy, University of Toronto, Toronto, ON, Canada

[3]Department of Surgery, Division of Anatomy, University of Toronto, Toronto, ON, Canada

[4]Institute of Biomaterials and Biomedical Engineering, University of Toronto, Toronto, ON, Canada

[5]Department of Molecular Genetics, University of Toronto, Toronto, ON, Canada

[6]Institute of Medical Science, University of Toronto, Toronto, ON, Canada

[7]Terrence Donnelly Centre for Cellular & Biomolecular Research, University of Toronto, Toronto, ON, Canada

[8]KITE, Toronto Rehabilitation Institute, University Health Network, Toronto, ON, Canada

Correspondence
Cindi M. Morshead, Institute of Medical Science, University of Toronto, Ontario, Canada.
Email: cindi.morshead@utoronto.ca

Funding information
Ontario Brain Institute; Canadian Institutes of Health Research; NeuroDevNet

Abstract

Neonatal stroke is a leading cause of long-term disability and currently available rehabilitation treatments are insufficient to promote recovery. Activating neural precursor cells (NPCs) in adult rodents, in combination with rehabilitation, can accelerate functional recovery following stroke. Here, we describe a novel method of constraint-induced movement therapy (CIMT) in a rodent model of neonatal stroke that leads to improved functional outcomes, and we asked whether the recovery was correlated with expansion of NPCs. A hypoxia/ischemia (H/I) injury was induced on postnatal day 8 (PND8) via unilateral carotid artery ligation followed by systemic hypoxia. One week and two weeks post-H/I, CIMT was administered in the form of 3 botulinum toxin (Botox) injections, which induced temporary paralysis in the unaffected limb. Functional recovery was assessed using the foot fault task. NPC proliferation was assessed using the neurosphere assay and EdU immunohistochemistry. We found that neonatal H/I injury alone expands the NPC pool by >2.5-fold relative to controls. We determined that using Botox injections as a method to provide CIMT results in significant functional motor recovery after H/I. However, CIMT does not lead to enhanced NPC activation or migration into the injured parenchyma in vivo. At the time of functional recovery, increased numbers of proliferating inflammatory cells were found within the injured motor cortex. Together, these findings suggest that NPC activation following CIMT does not account for the observed functional improvement and suggests that CIMT-mediated modification of the CNS inflammatory response may play a role in the motor recovery.

KEYWORDS

Botox, Constraint-induced movement therapy, neonatal hypoxia-ischemia, neural precursor cells, neuroplasticity, proliferation

[Correction added on 13 November 2020, after first online publication: The name of the second author was changed from Neemat D. Mahmud to Neemat Mahmud.]

Abbreviations: CIMT, Constraint-induced movement therapy; H/I, hypoxia-ischemia; NPC, neural precursor cell; PND, postnatal day.

Edited by Eilis Dowd

1 | INTRODUCTION

Neonatal stroke is a leading cause of motor and cognitive disability. With limited therapeutic interventions available, neonatal stroke often results in debilitating, non-progressive neurological deficits that persist throughout life, including cerebral palsy. One approach of considerable interest is the activation of endogenous neural stem cells and their progeny (neural precursor cells; NPCs), which are promising candidates to promote neural repair. NPCs reside in the periventricular region in the forebrain, through development and into adulthood (Morshead et al., 1994; Privat & Leblond, 1972; Smart, 1961; reviewed by Adams & Morshead, 2018). Under baseline conditions, NPCs migrate along the rostral migratory stream to the olfactory bulb where they differentiate into interneurons (Lois & Alvarez-Buylla, 1993; Lois et al., 1996; Craig et al., 1999). Following injury, the size of the activated NPC pool is increased (Dadwal et al., 2015; Sachewsky et al., 2014) and migration into the injured parenchyma is observed (Arvidsson et al., 2002; Faiz et al., 2015; Hou et al., 2008).

Studies have shown that injury-induced NPC activation alone is insufficient for tissue regeneration or functional recovery (Arvidsson et al., 2002; Kolb et al., 2007; Yamashita et al., 2006). However, further evidence reveals that enhancing endogenous NPCs activation through pharmacological approaches can promote sensorimotor and/or cognitive recovery in neonatal and adult stroke models (Dadwal et al., 2015; Erlandsson et al., 2011; Nusrat et al., 2018; Ruddy et al., 2019; Sachewsky et al., 2014). Further, it has been demonstrated that enriched rehabilitation, combined with endogenous NPC activation, leads to greater functional improvements than either intervention alone (Jeffers et al., 2014). It is well established that exercise promotes neurogenesis in the neurogenic regions of the brain (reviewed by Mastrorilli et al., 2017; Saraulli et al., 2017). These findings are consistent with the hypothesis that injury-induced NPC activation may be harnessed for activity-dependent neuroplasticity.

The prospect of modulating neurogenesis as a therapeutic intervention has garnered much interest from researchers, although the potential of the human brain to contribute to ongoing neurogenesis is controversial (Paredes et al., 2016; Sorrells et al., 2018). However, it is well-established that the developing neonatal brain affords greater plasticity, supports the survival, differentiation, and migration of NPCs, and guides nerve growth and synapse formation (reviewed by Adams & Morshead, 2018). Indeed, a marked decline in neurogenesis has been observed in both the SEZ and hippocampal neurogenic niches in early development and into aging through immunohistochemistry, immunofluorescence and stereology (Bhardwaj et al., 2006; Gould et al., 1999; Paredes et al., 2016; Sorrells et al., 2018). This suggests that a better opportunity for developing successful NPC-based recovery strategies is during the early postnatal period and that perhaps understanding and modulating neural precursor pools in early brain development is key to improving motor and cognitive outcomes in the context of neuronal injury during development and into adulthood.

Highlights

- Hypoxia-ischemia insult results in neural precursor cell (NPC) expansion for 1 week post-injury
- Botox is an effective model of constraint-induced movement therapy (CIMT)
- CIMT leads to functional gains in the absence of rehabilitation and enrichment
- CIMT mediated functional improvement is correlated with expansion of microglia/macrophages, but not the NPC pool at the time of recovery

Physical rehabilitation, including exercise and enriched environments, has long been used to improve motor function after stroke. In the case of neonatal stroke, paralysis and/or weakness affecting one side of the body (i.e. hemiplegia) can leads to repeated failed attempts to use the affected limb which results in "learned non-use," (Taub et al., 2006). A promising rehabilitative technique used in the clinic to overcome the discontinued use of an affected limb and increase use with the un-impaired limb is constraint-induced movement therapy (CIMT) (Taub et al., 1980; reviewed by Chiu & Ada, 2016; Livingston-Thomas et al., 2014; Uswatte & Taub, 2013). CIMT encourages positive feedback and modulates post-ischemic neuroplasticity through the restraint and immobilization of the unaffected arm and the forced use of the injured arm (Gillick & Zirpel, 2012; Ishida et al., 2015; Kim et al., 2015; Uswatte & Taub, 2013). Seminal work in rodent models (Taub, 1980, Taub, 2012; Taub et al., 2004), non-human primates, cerebral palsy and adult stroke patients (Carlson et al., 2018; Chen et al., 2016; Eliasson et al., 2018; Manning et al., 2016) and neonatal animal models (Ishida et al., 2015; Joo et al., 2012; Kim et al., 2017, 2018) indicates that CIMT leads to substantial functional improvements. However, the cellular mechanism responsible for the behavioural recovery is not well-understood. Herein, we asked whether enhancing an aspect of neuroplasticity—specifically NPC activation—is correlated with the success of CIMT to promote functional improvement in a neonatal H/I injury model. We established a novel method of CIMT using Botox to induce temporary paralysis in the unaffected paw following neonatal H/I and investigated changes in the NPC pool using in vitro and in vivo assays. We demonstrate that this CIMT strategy leads to motor improvements after neonatal stroke. We observed regionally distinct activation of microglia/macrophages but no evidence of SEZ NPC activation following CIMT treatment.

2 | MATERIALS AND METHODS

2.1 | Ethics Statement

All procedures were performed in accordance with the federal Canadian Council on Animal Care (CCAC) and the institutional University Animal Care Committee (UACC) at the University of Toronto.

2.2 | Mice

Gestational day 16-18 timed pregnant C57BL/6 female mice were purchased from Charles River and maintained in a pathogen-free facility. Litters of mice were housed with their dam in cages with a red rectangular house, one nestlet, and food and water available ad libitum. All mice were kept on a 12-hr day/night cycle. Dams were fed a high-fat diet (D12451, Charles River, Montreal, QC, Canada). Each litter (maximum of 8 pups/litter) included experimental mice and littermate controls of both sexes, which were randomly assigned to a treatment group (Naïve, Naïve + CIMT, H/I, H/I + CIMT).

2.3 | Hypoxia/ischemia (H/I) injury model

Early postnatal mice (postnatal day 8, PND8) received an H/I injury as previously described (Dadwal et al., 2015; Vannucci et al., 1999). Briefly, mice were anaesthetized (4% induction, 2% maintenance) with isoflurane (Fresenius-Kabi, Toronto, ON, Canada) and maintained on a heating pad at 37°C (ATC1000, World Precision Instruments, Sarasota, FL, USA). Under a dissecting microscope (T-22001, Ken-A-Vision, Kansas City, MO, USA), a midline ventral incision was made in the anterior neck and the left common carotid artery was ligated using 6–0 Sofsilk surgical sutures (VS-889, Syneture, Toronto, ON, Canada) and then cut between the sutures to permanently reduce blood flow. Following suturing, pups recovered under a heat lamp and returned to the dam for 1.5 hr. Pups were then exposed to 60 min of hypoxia in a sealed chamber (ProOx P110, Biospherix, Parish, NY, USA) infused with nitrogen until a level of 8.0% O2 is reached at 37°C. Following hypoxia exposure, pups were returned to the dam for recovery.

2.4 | CIMT (constraint-induced movement therapy) using botulinum toxin

Mice were anaesthetized with isoflurane (4% induction, 2% maintenance) and received botulinum toxin (Botox) (a kind gift from Allergan, ON, Canada) injections (0.05 u/μl in 1XPBS, 0.75 U/mouse) on PND15 and PND22. With a 34 gauge bevelled needle attached to a 100μl gastight syringe, 5μl of Botox was injected intramuscularly into the superior supraspinatus muscle, biceps brachii and triceps brachii. Mice were under anaesthesia for < 5 min from the time of induction to the time of the final injection. For mice receiving H/I + CIMT, only mice > 9gm on PND15 were used. Paralysis was visually observed (Supplemental Video 1). Mice that received CIMT dragged their paw and demonstrated decreased use (Supplemental Video 1). Paralysis was no longer apparent when observed 48 hr after the injection (Supplemental Video 2). All mice were frequently monitored and H/I + CIMT treated mice required more supportive care.

2.5 | Behavioural tasks

2.5.1 | Righting reflex

The Righting Reflex was a neurofunctional reflex used to demonstrate neural impairment in mice that received H/I injury. The time for pups to flip from a supine to prone position, (with a maximum time of 60 s) was assessed 1h after hypoxia on PND8 and compared to uninjured, naïve littermates that received anaesthesia, as done previously (El-Khodor et al., 2008; Ten et al., 2003). All mice that showed increased latency in the task were included in the study.

2.6 | Foot fault

To assess impairments in gross sensorimotor coordination and balance, and fine motor functions such as reaching and stepping, the Foot Fault task was performed (Bona et al., 1997; Lubics et al., 2005) at 4 days (PND26) and 13 days (PND35) after the final Botox injection, a time when the effects of Botox were no longer apparent (Video S2). Mice were placed on an elevated 1 cm x 1 cm grid and were allowed to explore for 3 min. The number of steps and the number of paw misplacements resulting in a slip through the grid ("faults") were recorded. To establish functional deficits and recovery, we measured the percent slippage and the percent faults/step. Percent slippage [(contralesional paw slips-ipsilesional paw slips)/total number of steps × 100%] was used to estimate gross motor coordination, specifically by assessing deficits between paws as a ratio. Another measure, percent faults per step, was used to assess paw-specific deficits [(i.e. right slips/right steps) × 100%].

2.7 | Neurosphere assay

Cohorts of mice were used to assess changes in neural stem cell numbers using the in vitro colony-forming

assay ("neurosphere" assay"), as described previously (Morshead et al., 2002). Briefly, mice were euthanized by a lethal overdose of sodium pentobarbital (54 mg/kg i.p.) followed by cervical dislocation. Neural stem cells were isolated by dissecting the periventricular regions from the medial and lateral walls and tissue was digested with enzymes (1.33 mg/ml trypsin, 0.67 mg/Ml hyaluronidase, and 0.2 mg/ml kynurenic acid, (Sigma-Aldrich, ON, Canada) for 25 min at 37°C. Cells were spun down and enzyme activity was inhibited with trypsin inhibitor (0.67 mg/ml, Worthington, NJ, USA). Tissue was mechanically dissociated into a single-cell suspension and plated at clonal density of 10 cells/µl (Coles-Takabe et al., 2008) in 24-well Nunc polystyrene plates (Thermo Fisher Scientific, IL, USA) in serum-free media (SFM) containing 1% penicillin/streptomycin (Invitrogen, ThermoFisher, ON, Canada), epidermal growth factor (20 ng/ml, Sigma-Aldrich, ON, Canada), basic fibroblast growth factor (10 ng/ml, Sigma-Aldrich, ON, Canada), and heparin (7.35 ng/ml, Sigma-Aldrich, ON, Canada). Cells were plated into 4 wells per mouse per treatment, and neurospheres ≥ 80µm in diameter were quantified 7 days after the dissection.

2.8 | Tissue preparation and immunohistochemistry

To examine cell proliferation, mice were injected once daily with 5-ethynyl-2′-deoxyuridine (EdU, Thermo Fisher Scientific, ON, Canada) at a dose of 25mg/kg (i.p.). Mice were sacrificed using a lethal overdose of sodium pentobarbital (54 mg/kg i.p.) 2 hr after the EdU injection, then transcardially perfused with cold 1X phosphate-buffered saline (PBS) followed by 4% paraformaldehyde (PFA). The brains were extracted and post-fixed in 4% PFA overnight, then cryoprotected in 30% sucrose for cryosectioning. Coronal sections (20 µm thick) were collected and mounted on Superfrost Plus slides from the genu of the corpus callosum to the crossing of the anterior commissure.

Slides were thawed at room temperature and rehydrated with 1XPBS. Sections were immunostained for EdU (Alexa Fluor 555 antibody) to assess for cell proliferation using the Invitrogen Molecular Probes Click-It EdU reaction kit (ThermoFisher, ON, Canada) as per manufacturer instructions. For all staining, slides were incubated with blocking solution containing 5% normal goat serum donkey serum in 1 X PBS + 0.5% Triton-X (Sigma-Aldrich, ON, Canada) + 1% BSA (Sigma-Aldrich, ON, Canada) for 1 hr at room temperature. Blocking solution was replaced with primary antibodies to assess markers for microglia/macrophages (Iba1, 1:500, Wako, 019–19171) and migrating neuroblasts (doublecortin/DCX, 1:250 Abcam, AB18723) and were incubated overnight at 4°C. The following day, slides were rinsed 3 × 5 min in 1 X PBS followed by incubation with secondary antibody (1:400 goat-anti-rabbit 488, Invitrogen, CA) for one hour at room temperature. Slides were rinsed 3 × 5 min in 1 X PBS 5 min and incubated in the presence of 1:10,000 DAPI (Invitrogen, CA). Following a final 5 min rinse in 1 X PBS, slides were coverslipped using Dako fluorescent mounting media (ThermoFisher, PA).

A minimum of three sections per brain were quantified and reported as the average number per unit area. An area of 500 µm × 500 µm was quantified in the periventricular region surrounding the ventricles; an area 1000 µm × 1000 µm was quantified in the striatum and cortex; a 1000 µm × 2000 µm area of the dentate gyrus was sampled in the hippocampus.

2.9 | Imaging and microscopy

A Zeiss Observer D1 inverted microscope was used to visualize immunofluorescence using GFP (488 nm excitation; 525 emission filter) and DsRed (555 nm excitation; 586 emission filter). Images were acquired at the 20x objective using Axio Vision (version 4.8.1.0).

2.10 | Statistical analysis

Data were analysed using Prism Software (GraphPad, Version 6). A Kruskal–Wallis test was used to assess changes in neurospheres. A Mann–Whitney test was used to analyse the righting reflex comparisons. Data collected during tissue analysis and the foot fault test were normally distributed, as determined by Shapiro–Wilk normality tests and a two-way analysis of variance (ANOVA) was used for multiple group comparisons when hemispheres were separated, followed by Bonferroni's post-hoc test. A one-way ANOVA was used for multiple group comparisons when hemispheres were combined, followed by Bonferroni's post-hoc test.

3 | RESULTS

3.1 | Hypoxia/Ischemia injury results in sensorimotor deficits and expands the NPC pool following injury

To assess the effectiveness of the H/I injury, sensorimotor deficits were evaluated early post-injury. H/I was performed as previously described (Dadwal et al., 2015) via unilateral ligation of the left common carotid artery followed by

1 hr of systemic hypoxia (Figure 1a) in PND8 mice. Mice were tested in the righting reflex task (Figure 1b) 1-hr post-hypoxia. Injured mice displayed a significantly increased latency to perform the righting reflex (14.5 ± 3.0 s versus 1.3 ± 0.2 s; injured versus uninjured animals, $n = 35$ and 16 mice, respectively), validating the injury model.

Given previous work showing that ischemic injury leads to increased neurogenesis in the postnatal brain periventricular region (Rah et al., 2011; Yang & Levison, 2006; Yang et al., 2007), we asked if neural stem cells (the earlier cell in the lineage) were similarly activated following H/I. We examined the size of the neural stem cell pool using the clonal,

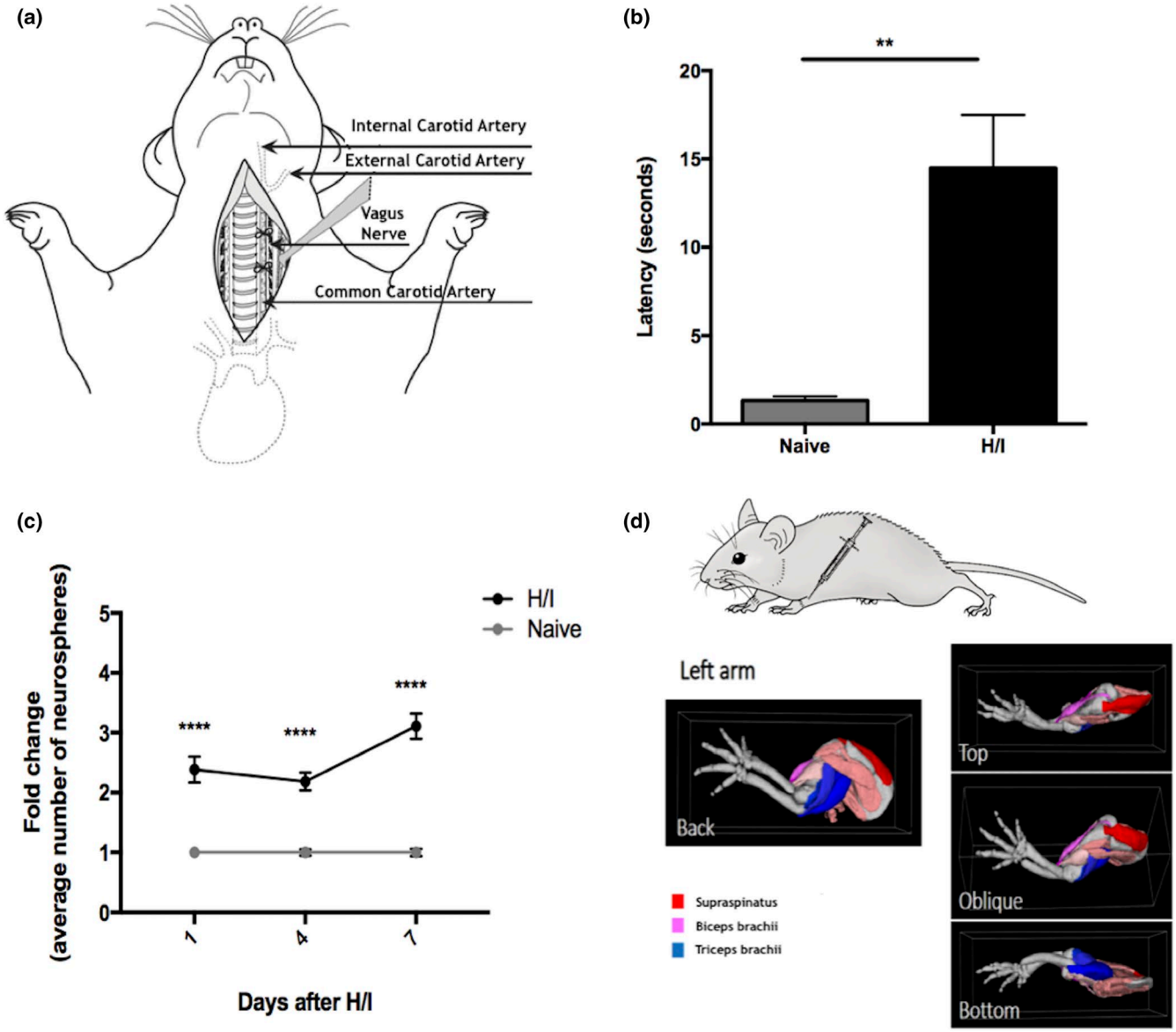

FIGURE 1 Neonatal hypoxia-ischemia (H/I) injury expands the NPC pool and Botox injections offer a novel method of constraint-induced movement therapy (CIMT). A. Schematic of the neonatal hypoxia-ischemia brain injury (Vannucci et al., 1992). Figure adapted from Nguyen et al., 2015 (https://doi.org/10.1007/978-1-4939-2709-8_1). B. Righting reflex performance in H/I injured mice relative to age-matched control mice that received isoflurane only. The amount of time in which mice were able to flip from supine position to prone position (with a maximum time of 60 s) was assessed one hour after recovering from anesthesia on PND8. H/I injured animals demonstrated a significant deficit in this task and these mice were used for long-term behaviour studies. Data are represented as mean ± *SEM*, unpaired *t*-test, $p = .005$, $n = \geq 16$ mice/group. C. Neurosphere numbers of H/I-injured mice relative to naïve mice at 1 day, 4 days, and 7 days post-H/I. Cells were plated in SFM + EFH at 2,500 cells/well into 4 wells per mouse per treatment, and neurospheres ≥ 80μm in diameter were quantified 7 days after the dissection. Neurosphere numbers were significantly increased in H/I injured animals relative to naïve mice at all times assessed. Data are represented as mean ± *SEM*, two-way ANOVA, $p = .03$, $n = \geq 6$ mice/group per time point. D. Schematic of Botox intramuscular injection delivery into the superior supraspinatus muscle, biceps and triceps to induce temporary paralysis in unaffected paw. Image adapted from the Mouse Limb Anatomy Atlas (http://www.nimr.mrc.ac.uk/3dlimb/)

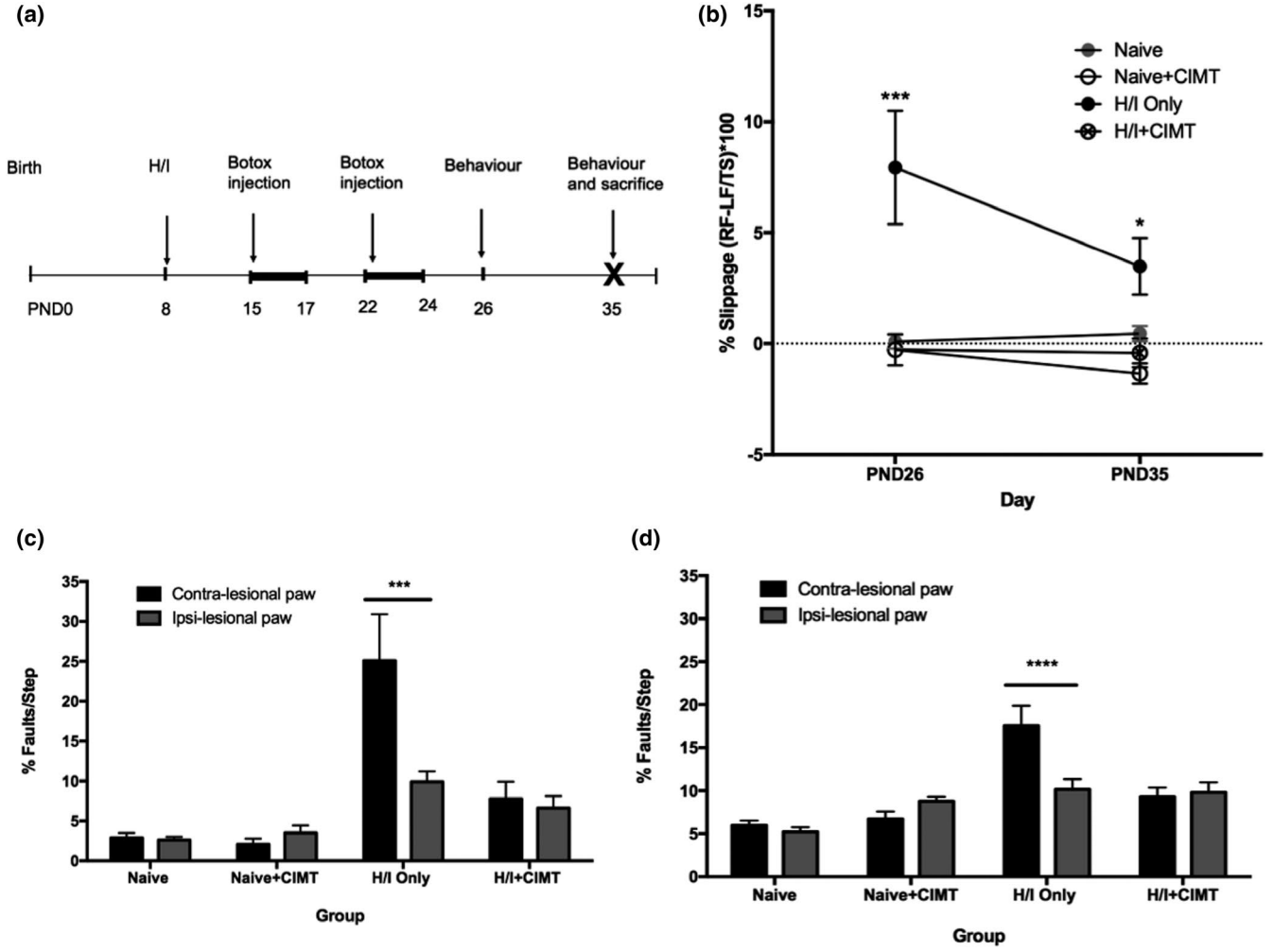

FIGURE 2 Treatment with CIMT results in motor recovery following H/I injury. A. Experimental paradigm investigating the potential for behavioural recovery using CIMT as a treatment for neonatal H/I injury. Gradients indicate the time of paralysis resulting from a single injection into the individual muscles and X denotes the time of sacrifice. B. Foot fault performance at short-term (PND26) and long-term (PND35) timepoints after CIMT (4 and 13 days after the second Botox injection). A significantly greater % Slippage was observed and maintained in mice that receive H/I only relative to all other groups. Data are represented as mean ± *SEM*, two-way ANOVA with Bonferroni correction, p=<0.0001, N = 3–12 mice per group, per time point. C., D. Foot fault performance at PND26 (C) and PND35 (D) separated by contralesional paw (i.e. right, paw, affected) and ipsilesional (i.e. left paw, Botox injected). H/I injured mice exhibit significant contralesional paw deficits. No significant difference in % Faults/Step between ipsilesional and contralesional paws was found in other groups. Data are represented as mean ± *SEM*, two-way ANOVA with Bonferroni correction, p=<0.0001, N = 3–12 mice per group, per time point

colony-forming neurosphere assay, whereby the numbers of neurospheres reflects the size of the neural stem cell pool (Morshead et al., 2002). Primary cultures of the postnatal periventricular region from injured and uninjured mice were plated in the neurosphere assay at 1, 4, and 7 days post-H/I. We observed a significant increase in neurosphere numbers from H/I injured mice, relative to control mice, at all times examined (2.3 ± 0.22 fold increase, 2.7 ± 0.15 fold increase, and 3.1 ± 0.21 fold increase at 1, 4, and 7 days post-H/I, respectively) (Figure 1c). Thus, the H/I injury alone is sufficient to increase the size of the NPC pool in the early postnatal brain for at least 1 week following injury.

3.2 | Constraint-induced movement therapy via botulinum toxin (BOTOX) leads to functional recovery post-H/I

Next, we established a model of CIMT in neonatal mice (Figure 2a). At one-week post-H/I—a time when significant NPC expansion was observed relative to naïve mice (Figure 1c)— Botox was delivered via intramuscular injection into the superior supraspinous, bicep and tricep muscles of the ipsilesional paw (ipsilesional to stroke injury) to induce temporary paralysis of the forelimb. Thus, Botox in the unaffected limb served as a restraint and promoted the use of the impaired

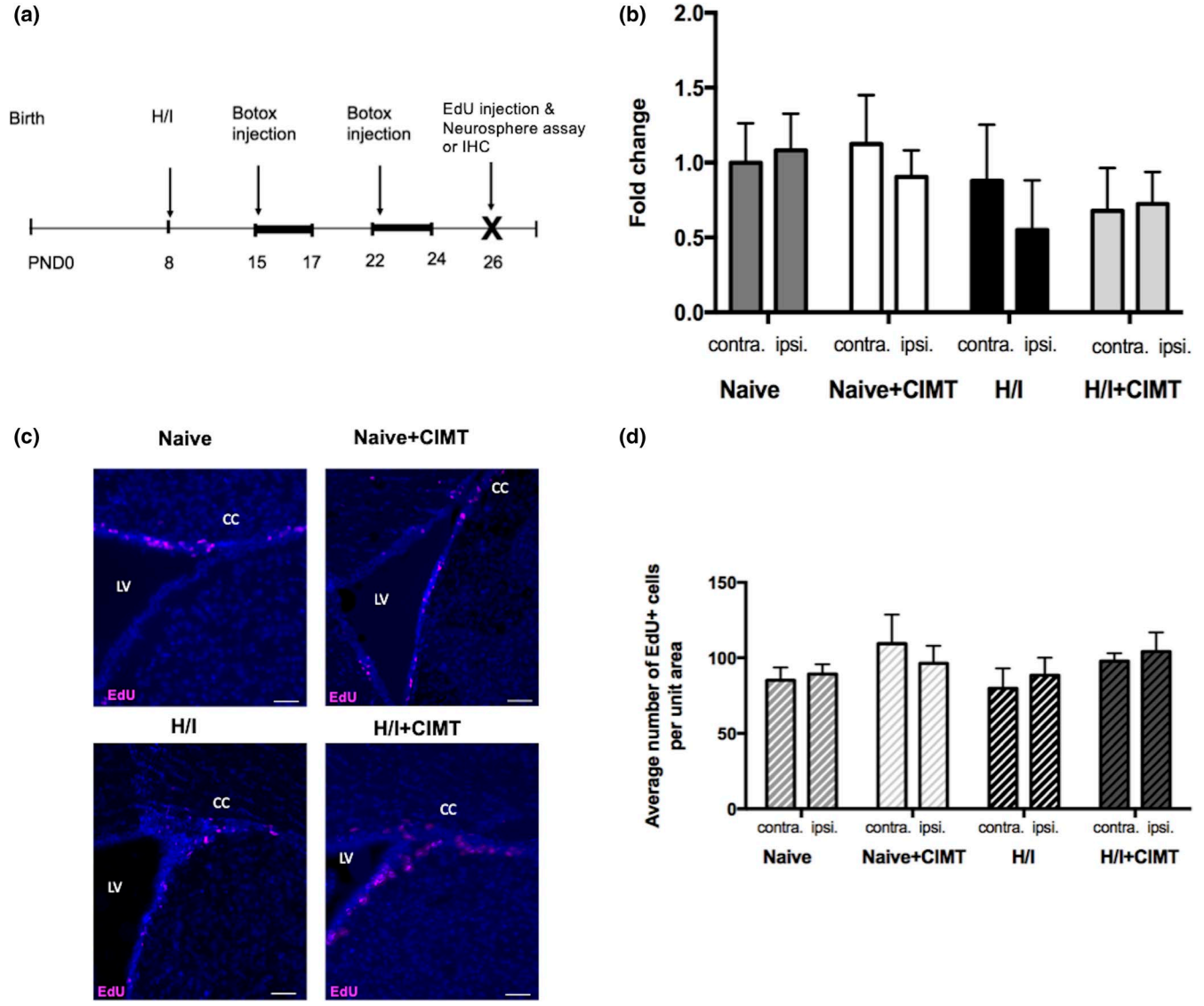

FIGURE 3 CIMT does not expand the endogenous NPC pool or increase proliferation in the periventricular region. A. Experimental paradigm investigating changes in the neurosphere numbers after CIMT. Gradients indicate the time of paralysis resulting from a single injection into the individual muscles and X denotes the time of sacrifice. B. Fold change in neurosphere numbers relative to naïve contralesional (right) hemisphere at PND26. No significant differences in the number of neurospheres were observed between hemispheres in mice that received CIMT (1.12 ± 0.33 versus 0.90 ± 0.18 fold change, contralesional versus ipsilesional, respectively), after injury (0.88 ± 0.37 versus 0.55 ± 0.33 fold change, contralesional versus ipsilesional, respectively) or after injury treated with CIMT (0.68 ± 0.29 versus 0.74 ± 0.21 fold change, contralesional versus ipsilesional, respectively) relative to naïve mice (1.00 ± 0.26 versus 1.08 ± 0.24 fold change, contralesional versus ipsilesional, respectively). No significant differences in the number of neurospheres were observed between treatment groups at PND26 in the contralesional hemisphere (Naive versus Naive + CIMT, $p = .98$; Naive versus H/I, $p = .98$; Naive versus H/I + CIMT, $p = .79$) or ipsilesional paw (Naive versus Naive + CIMT, $p = .94$; Naive versus H/I, $p = .46$; Naive versus H/I + CIMT, $p = .74$). Data are represented as mean ± *SEM*, $n = \geq 5$ mice/group per time point). C. Coronal sections depicting the dorsolateral corner of the lateral ventricle at PND26 immunostained for EdU + cells (pink) and DAPI (blue), scale bars = 50 µm. D. Percentage of EdU + cells within a 500 µm x 500 µm area of the in the periventricular region at PND26. Differences in proliferation were not observed between hemispheres in naïve mice at PND26 (85.2 ± 8.5 versus 89.4 ± 6.5 EdU + cells, contralesional versus ipsilesional, respectively), Naïve + CIMT (109.5 ± 19.2 versus 95.6 ± 11.5 EdU + cells contralesional versus ipsilesional, respectively), after H/I injury (79.78 EdU + cells±13.3 versus 88.4 ± 11.7 EdU + cells, contralesional versus.ipsilesional, respectively) or after H/I + CIMT (97.8 ± 5.3 versus 104.2 ± 12.7 EdU + cells, contralesional versus ipsilesional, respectively). No significant differences in the percentage of EdU + cells were observed between treatment groups at PND26 in either hemisphere (Naive versus CIMT only, $p = .54$ and $p = .99$ contralesional versus ipsilesional, respectively; Naive versus H/I, $p = .97$ and $p = .94$ contralesional versus ipsilesional, respectively; H/I versus H/I + CIMT, $p = .91$ and $p = .95$ contralesional versus ipsilesional, respectively). Data are represented as mean ± *SEM*, $n = \geq 3$ mice/group per time point

paw. Mice received Botox on PND15 and paralysis of the ipsilesional paw was visually observed (Video S1) until PND17, at which time they regained function in the Botox-injected limb. On PND22, mice received the same Botox regimen to induce a secondary temporary paralysis. Behavioural performance was assessed using the foot fault task at early time-points when the Botox induced paralysis was not observed (PND26, Figure 2c), and at a later time-point (PND35, Figure 2d) to examine the effectiveness of CIMT on motor function in naïve controls, H/I only, CIMT only, and H/I with CIMT. The percent slippage, which assessed inter-paw coordination as a ratio, was significantly greater in mice that receive H/I only compared to all other groups (7.9 ± 1.8 percent slippage, $p = .0003$) at PND26 and PND 35 (3.5 ± 1.1 percent slippage, $p = .022$). Similarly, when individual paws were assessed, mice that received H/I only compared to all other groups had a significantly increased %faults/step on their contralesional paw (7.9 ± 2.9 percent faults per step, $p = .0009$), which persisted to PND35 (3.5%±1.3, p=<0.0001), Importantly, no significant differences in % slippage were found between naïve mice and those that received H/I with CIMT, or CIMT only, suggesting that the CIMT is sufficient to improve functional outcomes following H/I injury, even in the absence of exercise, training, and environmental enrichment. Further, CIMT alone does not lead to sensorimotor deficits.

3.3 | CIMT does not expand the endogenous periventricular NPC pool or increase proliferation

We next sought to determine whether the successful CIMT induced recovery was correlated with NPC activation. In the first series of experiments, we performed the neurosphere assay at PND26, a time when functional recovery was observed (Figure 3a,b). We observed no significant differences in the number of neurospheres between treatment groups, in the contralesional hemisphere (Naive versus Naive + CIMT, $p = .98$; Naive versus H/I, $p = .98$; Naive versus H/I + CIMT, $p = .79$) or ipsilesional hemisphere (Naive versus Naive + CIMT, $p = .94$; Naive versus H/I, $p = .46$; Naive versus H/I + CIMT, $p = .74$), and no significant differences between hemispheres ($p = .88$). No significant differences were observed when hemispheres were combined ($p = .54$) (Figure S4a).

Potential NPC activation was further assessed by examining proliferation in the neurogenic regions of the postnatal brain in vivo. Mice received injections of EdU 2 hr prior to sacrifice on PND26 and the percentage of EdU + cells in the periventricular region was assessed using immunohistochemistry (Figure 3c, d). There were no significant differences in the numbers of EdU labelled cells in the periventricular regions between treatment groups at PND26 in the contralesional hemisphere (Naive versus CIMT only, $p = .14$; Naive versus H/I, $p = .94$; Naive versus H/I + CIMT, $p = .69$) or ipsilesional hemisphere (Naive versus Naïve, $p = .98$; Naive versus CIMT only, $p = .11$; Naive versus H/I, $p = .10$; Naive versus H/I + CIMT, $p = .24$), or between hemispheres ($p = .89$) (Figure 3c,d). No significant differences when hemispheres were combined ($p = .23$) (Figure S4b). Moreover, the total number of DAPI + cells across treatment groups was not different (Figure S2) ($p = .85$), suggesting the CIMT-mediated recovery was not due to increased cell survival in the periventricular region.

We examined the dentate gyrus of the hippocampus, another neurogenic region in the postnatal brain. Similarly, we

FIGURE 4 CIMT increases the proliferation of microglia/macrophages in the cortex, but not the striatum. A. Experimental paradigm. Gradients indicate the time of paralysis resulting from a single injection into the individual muscles and X denotes the time of sacrifice and tissue analysis (IHC = immunohistochemistry). B. Coronal sections through the striatum at PND26 immunostained for EdU + cells (pink) and DAPI (blue), scale bars = 50 μm. C. Average number of EdU+ cells within a 1,000 μm x 1,000 μm area of the striatum at PND26. Differences in proliferation were not observed between hemispheres (Supplemental Figure 3a) and hemispheres were combined for tissue analysis. No significant differences in the absolute number of EdU+ + cells observed between treatment groups (28.3 ± 3.7 EdU + cells in Naïve versus 20.7 ± 5.4 EdU + cells in Naive + CIMT versus 23.1 ± 7.2 EdU + cells after H/I injury versus 25.6 ± 6.3 EdU + cells in after H/I + CIMT, $p = .81$). Data are represented as mean ± *SEM*, $n = \geq 3$ mice/group per time point. D. Coronal sections through the cortex at PND26 immunostained for EdU + cells (pink) and DAPI (blue), scale bars = 50 μm. E. Average number of EdU+ cells within a 1,000 μm x 1,000 μm area of the cortex at PND26. Differences in proliferation were not observed between hemispheres (Supplemental Figure 3c) and hemispheres were combined for tissue analysis. There was a significant difference in the absolute number of EdU+ cells observed between treatment groups (11.7 ± 1.3 EdU+ cells in Naïve versus 10.3 ± 1.7 EdU + cells in Naive + CIMT versus 19.8 ± 3.1 EdU + cells after H/I injury versus 29.5 ± 4.0 EdU + cells in after H/I + CIMT, $p = .0003$). Data are represented as mean ± *SEM*, $n = \geq 3$ mice/group per time point. F. Coronal sections through the cortex at PND26 immunostained for Iba1+ (green)/EdU+ (pink) cells and DAPI (blue), scale bars = 50 μm. G. Average number of Iba1+/EdU+ cells within a 1,000 μm x 2000 μm area of the cortex at PND26. Differences in proliferation were not observed between hemispheres (Supplemental Figure 3d) and hemispheres were combined for tissue analysis. There was a significant difference in the absolute number of Iba1+/EdU + cells observed between treatment groups (19.0 ± 3.1 Iba1+/EdU+ cells in Naïve versus 12.9 ± 5.1 Iba1+/EdU+ cells in Naive + CIMT versus 21.5 ± 5.7 Iba1+/EdU+ cells after H/I injury versus 59.9 ± 11.4 Iba1+/EdU+ cells in after H/I + CIMT, $p = .0005$). The average number of Iba1+/EdU+ cells was statistically significant from all experimental groups. Data are represented as mean ± *SEM*, $n = \geq 3$ mice/group per time point

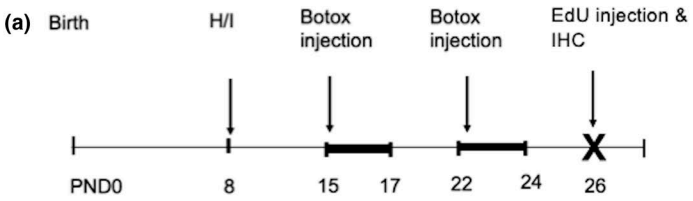
(a)
Birth
H/I
Botox injection
Botox injection
EdU injection & IHC
PND0
8
15
17
22
24
26

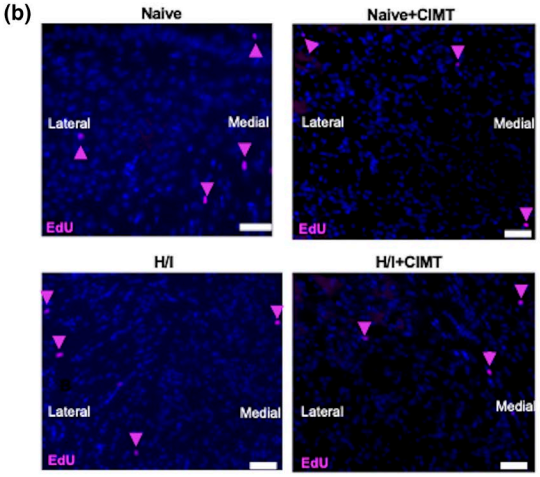
(b)
Naive
Naive+CIMT
H/I
H/I+CIMT
Lateral
Medial
EdU

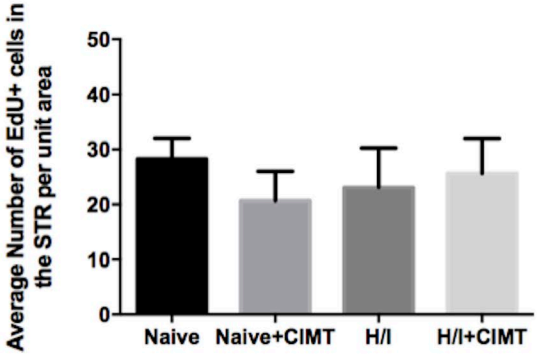
(c)
Average Number of EdU+ cells in the STR per unit area
0
10
20
30
40
50
Naive
Naive+CIMT
H/I
H/I+CIMT

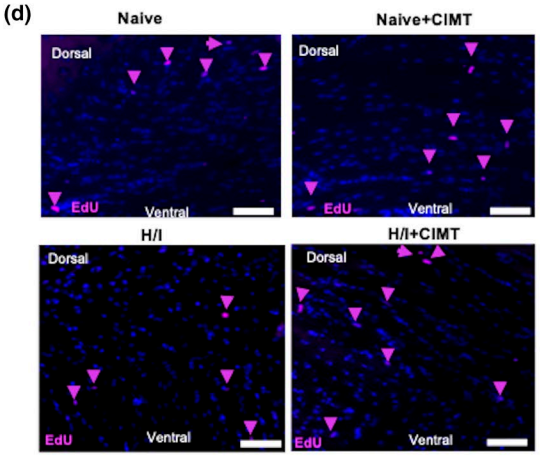
(d)
Naive
Naive+CIMT
H/I
H/I+CIMT
Dorsal
Ventral
EdU

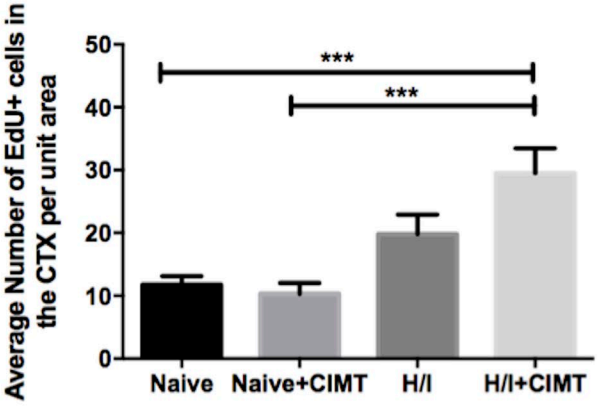
(e)
Average Number of EdU+ cells in the CTX per unit area
***
***
0
10
20
30
40
50
Naive
Naive+CIMT
H/I
H/I+CIMT

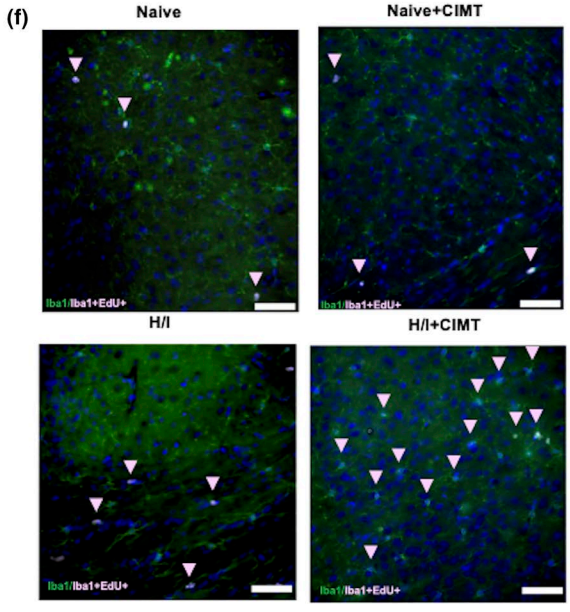
(f)
Naive
Naive+CIMT
H/I
H/I+CIMT
Iba1/Iba1+EdU+

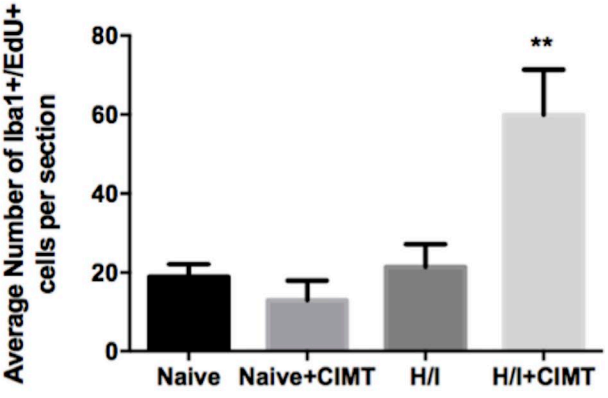
(g)
Average Number of Iba1+/EdU+ cells per section
**
0
20
40
60
80
Naive
Naive+CIMT
H/I
H/I+CIMT

observed no significant differences in proliferation (EdU+) between treatment groups at PND26 in the contralesional hemisphere (Naive versus CIMT only, p=>0.99; Naive versus H/I, p = .97; Naive versus H/I + CIMT, p = .95) or ipsilesional hemisphere (Naive versus Naïve, p=>0.99; Naive versus CIMT only, p=>0.99; Naive versus H/I, p=>0.99; Naive versus H/I + CIMT, p=>0.99) and no significant differences in the average numbers of EdU + cells between treatment groups (p = .91) (Figure S1).

3.4 | CIMT leads to a regionally distinct increase in proliferation in the cortex

In previous studies, we have shown that drug-mediated NPC activation can lead to functional motor recovery and that this is correlated with increased NPC activation in the neonatal stroke injured brain (Dadwal et al., 2015). Accordingly, we asked if the CIMT induced proliferation in the parenchyma, specifically in the striatum and the cortex which underlie motor function. We observed no difference in the numbers of proliferating cells between the ipsilateral and contralateral hemispheres in any group and the hemispheres were combined. A comparison between treatment groups revealed no significant differences in the numbers of EdU + cells in the striatum at PND26 (p = .81) (Figure 4b,c). Interestingly, we observed a significant increase in the numbers of EdU + cells in the cortex of mice that received H/I + CIMT (p = .003) (Figure 4d,e).

3.5 | CIMT does not increase the migration of the progeny of neural precursor cells

We next sought to determine if NPC progeny (neuroblasts, DCX+ cells) could account for the EdU+ cells within the parenchyma. We quantified the number of EdU+/DCX+ cells in the striatum, the cortex and the dentate gyrus. As shown in Figure 5, we found no differences in the number of EdU+/DCX+ cells across treatment groups in the striatum (p = .48) (Figure 5b,c), cortex (p = .43) (Figure 5d,e), or the dentate gyrus (p = .79) (Figure S1c). Hence, neuroblast migration was not occurring at the time of functional recovery in the CIMT-treated mice.

3.6 | CIMT increases the proliferation of microglia/macrophages in the cortex

This neonatal stroke model has been shown to induce an inflammatory response through the activation of Iba1+ cells (microglia and macrophages) (Hellström Erkenstam et al., 2016; Livingston et al., 2020; Serdar et al., 2019). With the goal of identifying the EdU+ cells that were expanded in the cortex of H/I + CIMT mice, we examined the numbers of Iba1+/EdU+ cells in the cortex of mice from each group. Interestingly, H/I + CIMT mice had significantly more Iba1+/EdU+ cells compared to all other groups (18.9 ± 3.1 Iba1+/EdU+cells in Naïve versus 12.9 ± 5.1 Iba1+/EdU+cells in Naive + CIMT versus 21.5 ± 5.7 Iba1+/EdU+cells after H/I injury versus 59.9 ± 11.4 Iba1+/EdU+cells in after H/I + CIMT, p = .0005). The increase in microglia/macrophage at the time when functional recovery is observed is consistent with the idea that immunomodulation in the injured cortex plays a role in the CIMT-mediated recovery.

Taken together, these findings suggest that the improved functional outcomes observed following successful CIMT treatment are independent of NPC expansion and proliferation at the time of observed recovery, and consistent with increased proliferation of microglia/macrophages in the cortex.

4 | DISCUSSION

Herein, we demonstrated that constraint-induced movement therapy (CIMT) is able to promote functional recovery in a neonatal mouse model of stroke. We show that the recovery is not correlated with an increase in neural precursor cell activation. We use a novel approach to induce temporary paralysis in neonatal mice using Botox injections, which allowed

FIGURE 5 CIMT does not increase the numbers of migrating neuroblasts found in the parenchyma. A. Coronal sections through the striatum at PND26 immunostained for DCX+ (green)/EdU+ cells (pink) and DAPI (blue), scale bars = 50 μm. B. The average numbers of DCX+/EdU+ cells within a 1,000 μm x 1,000 μm area of the striatum at PND26 revealed. Differences in proliferation were not observed between hemispheres (Supplemental Figure 3b) and hemispheres were combined for tissue analysis. No significant differences in the numbers of DCX+/EdU+ cells observed between treatment groups (28.3 ± 3.7 cells in Naïve versus 20.7 ± 5.4 cells in Naive + CIMT versus 23.1 ± 7.2 cells in H/I injury versus 25.6 ± 6.3 cells in H/I + CIMT, p = .81). Data are represented as mean ± *SEM*, n = ≥3 mice/group per time point. C. Coronal sections through the cortex at PND26 immunostained for DCX+ (green)/EdU+ cells (pink) and DAPI (blue), scale bars = 50 μm. D. The average number of DCX+/EdU+ cells within a 1,000 μm x 1,000 μm area of the cortex at PND26. Differences in proliferation were not observed between hemispheres (Supplemental Figure 3c) and hemispheres were combined for tissue analysis. There was a significant differences in the absolute number of DCX+/EdU+ cells observed between treatment groups (7.2 ± 1.3 DCX+/EdU+ cells in Naïve versus 8.7 ± 1.3 DCX+/EdU+ cells in Naive + CIMT versus 6.2 ± 0.7 DCX+/EdU+ cells after H/I injury versus 6.6 ± 0.9 EdU+ cells in after H/I + CIMT, p = .043). Data are represented as mean ± *SEM*, n = ≥3 mice/group per time point

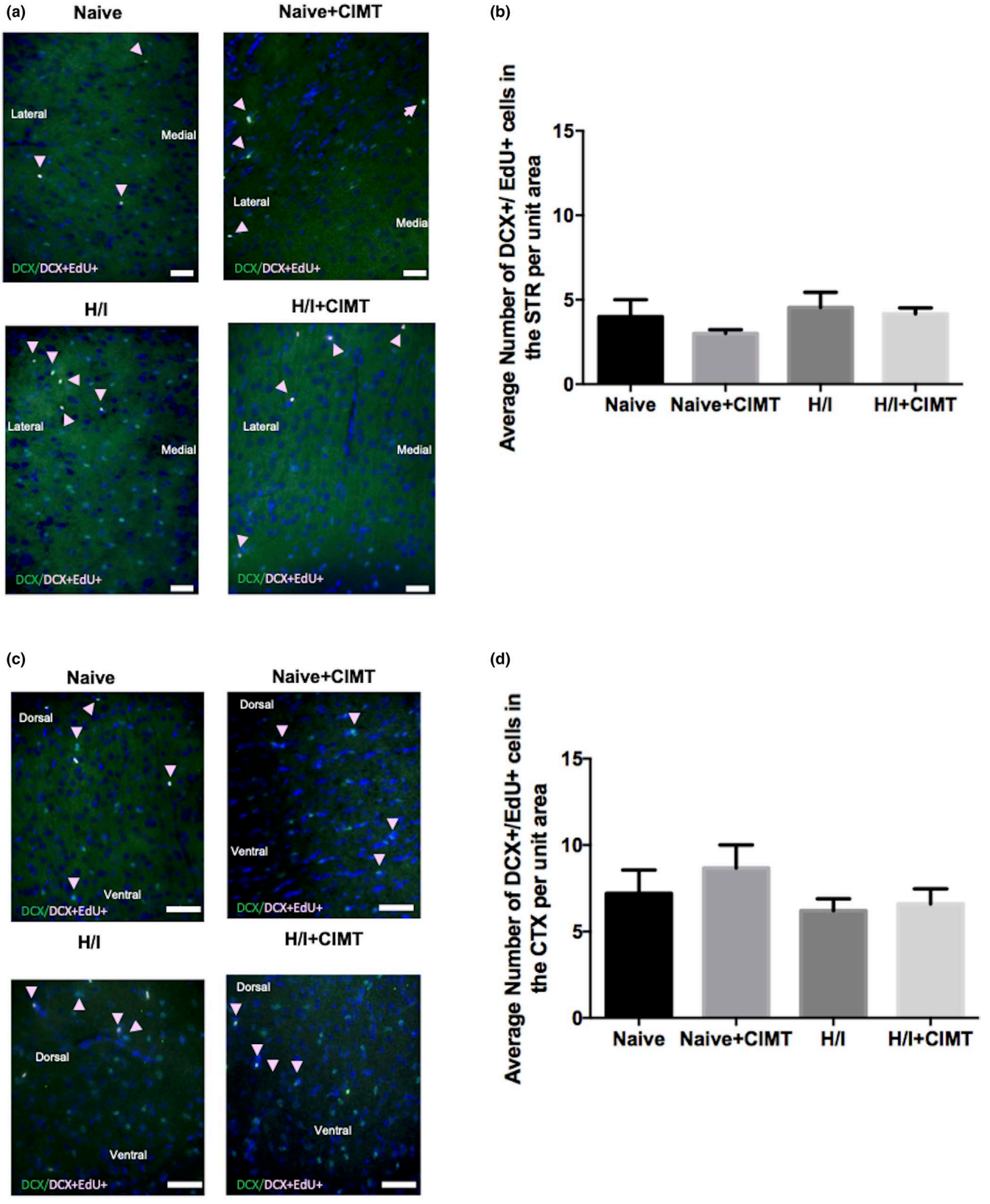

us to examine potential mechanisms of neuroplasticity that ultimately underlies the success of the treatment. We were most interested in changes in motor behaviour for this study and predicted that activation of endogenous NPCs derived from the SEZ may underlie the CIMT-mediated functional recovery. We found that NPC activation occurs as a result of the neonatal stroke injury (as seen with an expansion in the size of the neural stem cell pool), similar to what is

observed in adult stroke (Sachewsky et al., 2014); however, the functional recovery observed with CIMT treatment was not correlated with NPC mediated neuroplasticity. Our findings suggest that immunomodulation may play a role in the observed functional improvement.

CIMT is relatively non-invasive; however, modelling forced use in animals can be challenging (Livingston-Thomas & Tasker, 2013). Techniques that have been used to immobilize the unimpaired forelimb—such as casts, slings, jackets, adhesives, or devices—often leads to animals attempting to remove the restraint. Furthermore, physical restraints have been shown to elevate serum levels of glucocorticoid hormones, which can exacerbate ischemic injury (Ke et al., 2011) and worsen outcomes (Ishida et al., 2011). The increased stress levels with physical restraints is a major criticism of CIMT and neurorehabilitation in general. Here, we have demonstrated that immobilizing the un-impaired limb with Botox in juvenile mice can lead to motor improvements following neonatal stroke. This work builds on the recent studies by Lam et al., 2013, and Liang et al., 2019, that reported the use of Botox to immobilize the forelimb in adult animals using a different injury model. We are the first to use this strategy in juvenile animals following neonatal brain injury, and we modified the technique to enable paralysis with fewer injection sites per limb. We propose that this paradigm of Botox-induced CIMT offers an effective, less-invasive method of forelimb restraint for the purpose of neurorehabilitation with the absence of a visual cue normally associated with forced use.

A number of studies report that CIMT alone is insufficient for functional recovery, and suggest that CIMT needs to be paired with daily rehabilitation exercises (Debow et al., 2003; Jeffers et al., 2014; Kim et al., 2018), and/or highly social environments (Kim et al., 2018; Rha et al., 2011), in order to contribute to significant motor gains (Debow et al., 2003; Jeffers et al., 2014; Kim et al., 2018). Indeed, studies showing that combinatorial strategies are more effective than single interventions have been reported. For instance, pharmacotherapeutic activation of NPCs combined with rehabilitation is more effective than either strategy alone to treat stroke-injured rats (Jeffers et al., 2014; Kim et al., 2018; Zhao et al., 2009). We observed that constraint without rehabilitation was sufficient to produce significant functional improvements, although it is likely that motor function could be even further enhanced with exercise, training and pharmacotherapy (Jeffers et al., 2014; Livingston-Thomas & Tasker, 2013).

Although our findings that CIMT promotes behavioural recovery are well-supported by clinical findings and animal studies, our findings are not consistent with previous reports that CIMT increases neurogenesis (Ishida et al., 2015; Rha et al., 2011; Zhang et al., 2001; Zhao et al., 2009, 2013; Zhao, Zhao, Xiao, Zhao, et al., 2013) and enhances cell survival (Kim et al., 2018; Zhang et al., 2013b). Differences that could account for the discrepancies include the animal model of injury and duration of CIMT (plaster cast and for 2 continuous weeks), as well as the paradigm for labelling proliferating cells, the region analysed and functional outcome measured (rotarod, grip strength task, and the horizontal ladder rung) (Liu et al., 2019; Qu et al., 2015; Rha et al., 2011; Zhao et al., 2009; Zhao, Zhao, Xiao, Jolkkonen, et al., 2013; Zhao, Zhao, Xiao, Zhao, et al., 2013). A limitation of our study is that while we did not observe changes in the numbers of proliferating (EdU+) cells between treatment groups, we observed very few EdU+ cells in the parenchyma, suggesting that the activated SEZ-derived NPCs may have continued to proliferate in situ after their migration to the parenchyma. We cannot rule out the possibility we missed the window of NPC proliferation/activation, or that EdU was diluted by the time we examined the tissue, given that the cell cycle time for neuroblasts in 8-week old adult mice is approximately 18 hr (Ponti et al., 2013), and neonates may have a more rapid cell cycle time. Another possibility is that the window of NPC activation occurred earlier than when we performed the tissue analyses and we propose that that lineage tracing experiments would offer further insight. Other potential mechanisms underlying the use-dependent recovery could be related increased synaptogenesis (Liang et al., 2019; Zhao, Zhao, Xiao, Jolkkonen, et al., 2013; Zhao, Zhao, Xiao, Zhao, et al., 2013), increased axonal growth (Ishida et al., 2015; Zhao, Zhao, Xiao, Jolkkonen, et al., 2013; Zhao, Zhao, Xiao, Zhao, et al., 2013) and/or cortical reorganization (Kuo et al., 2018; Liang et al., 2019; Sawaki et al., 2014; Taub et al., 2014; Xerri et al., 2014). Understanding the mechanisms will provide important insight into novel approaches to promote neural repair.

In this study, we observed an increase in activated (proliferative) inflammatory cells in mice that received CIMT and demonstrated functional recovery. Microglia, the resident immune cells of the brain, have been shown to contribute to CNS development and maintenance under baseline conditions, and play a critical role in removing debris and restoring tissue homeostasis after injury (reviewed by Lloyd & Miron, 2019; Vay et al., 2018). After neonatal H/I injury, microglia increase in number as early as 6 hr following injury and express elevated levels of pro-inflammatory cytokines (e.g.; TNF-α, IL-1β and IL-6) (Tay et al., 2017). Interestingly, we have recently demonstrated that neonatal H/I injury leads to increased numbers of microglia/macrophages for at least 21 days after injury and that the delivery of therapeutics that lead to functional improvement (specifically the administration of the drug metformin) can decrease the microglia/macrophage response (Livingston et al., 2020; Aarum et al., 2003). There is also evidence that cerebral ischemia results in sustained neuroinflammation for months following stroke and that the removal of degenerating tissue and release of

anti-inflammatory cytokines (e.g.; IL-10, TFGβ) can promote neuroprotection, remyelination, axonal regeneration and stem cell-mediated tissue repair (Lloyd & Miron, 2019). Taken together, this suggests that harnessing the plasticity of microglia is a potential target for functional recovery of the neonatal stroke-injured brain.

5 | CONCLUSION

We have demonstrated the efficacy of Botox as a method of inducing CIMT that is sufficient to promote motor recovery in a model of neonatal stroke, with no concomitant expansion of NPCs, but an observed immune cell activation in the cortex. Elucidating the mechanism of how CIMT promotes recovery remains a challenge in the field. Important studies to determine a causal link between CIMT, neurogenesis, neuroplasticity and improved behavioural performance will facilitate the development of novel therapies to promote neural repair.

ACKNOWLEDGEMENTS

This work was supported by funding from the Ontario Brain Institute, NeuroDevNet, and CIHR. We thank Mandy Yee for assisting with video scoring and Samantha Yammine for assisting with supportive care. We thank Allergan for providing the Botox used in these studies. We thank the Morshead lab members for their feedback on the manuscript.

CONFLICT OF INTERESTS

The authors declare that there is no conflict of interest.

AUTHOR CONTRIBUTIONS

K.A. performed neurosphere assays, immunohistochemistry, tissue analysis, imaging, and quantification, assembled, analysed, interpreted data, prepared, wrote and approved the manuscript. N.M. performed surgeries and neurosphere assays and quantified immunohistochemistry and data analyses. M.G-H. contributed to tissue analysis, imaging and quantification. I.V. performed foot-fault analysis. D.U. designed the Botox paradigm of the CIMT strategy used, performed Botox injections and performed data analysis. NS performed surgeries and Botox injections and B.C-T. provided supportive care and technical support. D.VDK and C.M.M conceived and designed the study, provided financial support, analysed and interpreted data, and wrote and gave final approval of the manuscript.

DATA AVAILABILITY STATEMENT

Supporting data and materials were made available with this manuscript submission.

PEER REVIEW

The peer review history for this article is available at https://publons.com/publon/10.1111/ejn.14993.

ORCID

Kelsey V. Adams https://orcid.org/0000-0003-1407-5743

REFERENCES

Aarum, J., Sandberg, K., Haeberlein, S. L. B., & Persson, M. A. A. (2003). Migration and differentiation of neural precursor cells can be directed by microglia. *Proceedings of the National Academy of Sciences of the USA*, *100*, 15983–15988.

Adams, K. V., & Morshead, C. M. (2018). Neural stem cell heterogeneity in the mammalian forebrain. *Progress in Neurobiology*, *170*, 2–36.

Arvidsson, A., Collin, T., Kirik, D., Kokaia, Z., & Lindvall, O. (2002). Neuronal replacement from endogenous precursors in the adult brain after stroke. *Nature Medicine*, *8*, 963–970. https://doi.org/10.1038/nm747

Bhardwaj, R. D., Curtis, M. A., Spalding, K. L., Buchholz, B. A., Fink, D., Bjork-Eriksson, T., Nordborg, C., Gage, F. H., Druid, H., Eriksson, P. S., & Frisen, J. (2006). Neocortical neurogenesis in humans is restricted to development. *Proceedings of the National Academy of Sciences of the USA*, *103*, 12564–12568. https://doi.org/10.1073/pnas.0605177103

Bona, E., Johansson, B. B., & Hagberg, H. (1997). Sensorimotor function and neuropathology five to six weeks after hypoxia-ischemia in seven-day-old rats. *Pediatric Research*, *42*, 678–683. https://doi.org/10.1203/00006450-199711000-00021

Carlson, H. L., Ciechanski, P., Harris, A. D., MacMaster, F. P., & Kirton, A. (2018). Changes in spectroscopic biomarkers after transcranial direct current stimulation in children with perinatal stroke. *Brain Stimulation*, *11*, 94–103. https://doi.org/10.1016/j.brs.2017.09.007

Chen, H. C., Kang, L. J., Chen, C. L., Lin, K. C., Chen, F. C., & Wu, K. P. H. (2016). Younger children with cerebral palsy respond better than older ones to therapist-based constraint-induced therapy at home on functional outcomes and motor control. *Physical & Occupational Therapy in Pediatrics*, *36*, 171–185. https://doi.org/10.3109/01942638.2015.1101042

Chiu, H. C., & Ada, L. (2016). Constraint-induced movement therapy improves upper limb activity and participation in hemiplegic cerebral palsy: A systematic review. *Journal of Physiotherapy*, *62*, 130–137. https://doi.org/10.1016/j.jphys.2016.05.013

Coles-Takabe, B. L. K., Brain, I., Purpura, K. A., Karpowicz, P., Zandstra, P. W., Morshead, C. M., & Van der Kooy, D. (2008). Don't look: Growing clonal versus nonclonal neural stem cell colonies. *Stem Cells*, *26*, 2938–2944. https://doi.org/10.1634/stemcells.2008-0558

Craig, C. G., D'Sa, R., Morshead, C. M., Roach, A., & Van der Kooy, D. (1999). Migrational analysis of the constitutively proliferating subependyma population in adult mouse forebrain. *Neuroscience*, *93*, 1197–1206. https://doi.org/10.1016/S0306-4522(99)00232-8

Dadwal, P., Mahmud, N., Sinai, L., Azimi, A., Fatt, M., Wondisford, F. E., Miller, F. D., & Morshead, C. M. (2015). Activating endogenous neural precursor cells using metformin leads to neural repair and functional recovery in a model of childhood brain injury. *Stem Cell Reports*, *5*, 166–173. https://doi.org/10.1016/j.stemcr.2015.06.011

DeBow, S. B., Davies, M. L. A., Clarke, H. L., & Colbourne, F. (2003). Constraint-induced movement therapy and rehabilitation exercises lessen motor deficits and volume of brain injury after striatal hemorrhagic stroke in rats. *Stroke*, *34*, 1021–1026. https://doi.org/10.1161/01.STR.0000063374.89732.9F

Eliasson, A. C., Nordstrand, L., Ek, L., Lennartsson, F., Sjostrand, L., Tedroff, K., & Krumlinde-Sundholm, L. (2018). The effectiveness of Baby-CIMT in infants younger than 12 months with clinical signs of unilateral-cerebral palsy; an explorative study with randomized design. *Research in Developmental Disabilities*, *72*, 191–201. https://doi.org/10.1016/j.ridd.2017.11.006

El-Khodor, B. F., Edgar, N., Chen, A., Winberg, M. L., Joyce, C., Brunner, D., Suarez-Farinas, M., & Heyes, M. P. (2008). Identification of a battery of tests for drug candidate evaluation in the SMN Delta 7 neonate model of spinal muscular atrophy. *Experimental Neurology*, *212*, 29–43.

Erlandsson, A., Lin, C. H. A., Yu, F. G., & Morshead, C. M. (2011). Immunosuppression promotes endogenous neural stem and progenitor cell migration and tissue regeneration after ischemic injury. *Experimental Neurology*, *230*, 48–57.

Faiz, M., Sachewsky, N., Gascon, S., Bang, K. W. A., Morshead, C. M., & Nagy, A. (2015). Adult neural stem cells from the subventricular zone give rise to reactive astrocytes in the cortex after stroke. *Cell Stem Cell*, *17*, 624–634. https://doi.org/10.1016/j.stem.2015.08.002

Gillick, B. T., & Zirpel, L. (2012). Neuroplasticity: An appreciation from synapse to system. *Archives of Physical Medicine and Rehabilitation*, *93*, 1846–1855.

Gould, E., Reeves, A. J., Graziano, M. S. A., & Gross, C. G. (1999). Neurogenesis in the neocortex of adult primates. *Science*, *286*, 548–552. https://doi.org/10.1126/science.286.5439.548

Hellström Erkenstam, N., Smith, P. L. P., Fleiss, B., Nair, S., Svedin, P., Wang, W., Boström, M., Gressens, P., Hagberg, H., Brown, K. L., Sävman, K., & Mallard, C. (2016). Temporal characterization of microglia/macrophage phenotypes in a mouse model of neonatal hypoxic-ischemic brain injury. *Frontiers in Cellular Neuroscience*, *10*, 286. https://doi.org/10.3389/fncel.2016.00286

Hou, S. W., Wang, Y. Q., Xu, M., Shen, D. H., Wang, J. J., Huang, F., Yu, Z., & Sun, F. Y. (2008). Functional integration of newly generated neurons into striatum after cerebral ischemia in the adult rat brain. *Stroke*, *39*, 2837–2844. https://doi.org/10.1161/STROKEAHA.107.510982

Ishida, A., Misumi, S., Ueda, Y., Shimizu, Y., Cha-Gyun, J., Tamakoshi, K., Ishida, K., & Hida, H. (2015). Early constraint-induced movement therapy promotes functional recovery and neuronal plasticity in a subcortical hemorrhage model rat. *Behavioural Brain Research*, *284*, 158–166.

Ishida, A., Ueda, Y., Ishida, K., Misumi, S., Masuda, T., Fujita, M., & Hida, H. (2011). Minor neuronal damage and recovered cellular proliferation in the hippocampus after continuous unilateral forelimb restraint in normal rats. *Journal of Neuroscience Research*, *89*, 457–465.

Jeffers, M. S., Hoyles, A., Morshead, C., & Corbett, D. (2014). Epidermal growth factor and erythropoietin infusion accelerate functional recovery in combination with rehabilitation. *Stroke*, *45*, 1856–1858. https://doi.org/10.1161/STROKEAHA.114.005464

Joo, H. W., Hyun, J. K., Kim, T. U., Chae, S. H., Lee, Y. I., & Lee, S. J. (2012). Influence of constraint-induced movement therapy upon evoked potentials in rats with cerebral infarction. *European Journal of Neuroscience*, *36*, 3691–3697.

Kim, H., Kim, M. J., Koo, Y. S., Lee, H. I., Lee, S. W., Shin, M. J., Kim, S. Y., Shin, Y. B., Shin, Y. I., Choi, B. T., Yun, Y. J., & Shin, H. K. (2017). Histological and functional assessment of the efficacy of constraint-induced movement therapy in rats following neonatal hypoxic-ischemic brain injury. *Experimental and Therapeutic Medicine*, *13*, 2775–2782. https://doi.org/10.3892/etm.2017.4371

Kim, H., Koo, Y. S., Shin, M. J., Kim, S. Y., Shin, Y. B., Choi, B. T., Yun, Y. J., Lee, S. Y., & Shin, H. K. (2018). Combination of constraint-induced movement therapy with electroacupuncture improves functional recovery following neonatal hypoxic-ischemic brain injury in rats. *BioMed Research International*, *2018*, 8638294.

Kim, S. Y., Allred, R. P., Adkins, D. L., Tennant, K. A., Donlan, N. A., Kleim, J. A., & Jones, T. A. (2015). Experience with the "good" limb induces aberrant synaptic plasticity in the perilesion cortex after stroke. *Journal of Neuroscience*, *35*, 8604–8610.

Kolb, B., Morshead, C., Gonzalez, C., Kim, M., Gregg, C., Shingo, T., & Weiss, S. (2007). Growth factor-stimulated generation of new cortical tissue and functional recovery after stroke damage to the motor cortex of rats. *Journal of Cerebral Blood Flow and Metabolism*, *27*, 983–997.

Kuo, H. C., Zewdie, E., Ciechanski, P., Damji, O., & Kirton, A. (2018). Intervention-induced motor cortex plasticity in hemiparetic children with perinatal stroke. *Neurorehabilitation and Neural Repair*, *32*, 941–952. https://doi.org/10.1177/1545968318801546

Lam, T. I., Bingham, D., Chang, T. J., Lee, C. C., Shi, J., Wang, D. M., Massa, S., Swanson, R. A., & Liu, J. L. (2013). Beneficial effects of minocycline and botulinum toxin-induced constraint physical therapy following experimental traumatic brain injury. *Neurorehabilitation and Neural Repair*, *27*, 889–899. https://doi.org/10.1177/1545968313491003

Liang, H., Zhao, H., Gleichman, A., Machnicki, M., Telang, S., Tang, S., Rshtouni, M., Ruddell, J., & Carmichael, S. T. (2019). Region-specific and activity-dependent regulation of SVZ neurogenesis and recovery after stroke. *Proceedings of the National Academy of Sciences of the USA*, *116*, 13621–13630.

Liu, X. H., Bi, H. Y., Cao, J., Ren, S., & Yue, S. W. (2019). Early constraint-induced movement therapy affects behavior and neuronal plasticity in ischemia-injured rat brains. *Neural Regeneration Research*, *14*, 775–782.

Livingston, J., Syeda, T., Christie, T., Gilbert, E., & Morshead, C. (2020). Subacute metformin treatment reduces inflammation and improves functional outcome following neonatal hypoxia ischemia. *Brain, Behavior, & Immunity - Health*, *2020*, https://doi.org/10.1016/j.bbih.2020.100119

Livingston-Thomas, J. M., Hume, A. W., Doucette, T. A., & Tasker, R. A. (2013). A novel approach to induction and rehabilitation of deficits in forelimb function in a rat model of ischemic stroke. *Acta Pharmacologica Sinica*, *34*, 104–112.

Livingston-Thomas, J. M., McGuire, E. P., Doucette, T. A., & Tasker, R. A. (2014). Voluntary forced use of the impaired limb following stroke facilitates functional recovery in the rat. *Behavioural Brain Research*, *261*, 210–219.

Lloyd, A. F., & Miron, V. E. (2019). The pro-remyelination properties of microglia in the central nervous system. *Nature Reviews Neurology*, *15*, 447–458.

Lois, C., & Alvarezbuylla, A. (1993). Proliferating subventricular zone cells in the adult mammalian forebrain can differentiate into neurons and glia. *Proceedings of the National Academy of Sciences of the USA*, *90*, 2074–2077.

Lois, C., & Alvarez-Buylla, A. (1994). Long-distance neuronal migration in the adult mammalian brain. *Science*, *264*, 1145–1148. https://doi.org/10.1126/science.8178174

Lubics, A., Reglodi, D., Tamas, A., Kiss, P., Szalai, M., Szalontay, L., & Lengvari, I. (2005). Neurological reflexes and early motor behavior in rats subjected to neonatal hypoxic-ischemic injury. *Behavioural Brain Research*, *157*, 157–165.

Manning, K. Y., Menon, R. S., Gorter, J. W., Mesterman, R., Campbell, C., Switzer, L., & Fehlings, D. (2016). Neuroplastic sensorimotor resting state network reorganization in children with hemiplegic cerebral palsy treated with constraint-induced movement therapy. *Journal of Child Neurology*, *31*, 220–226.

Mastrorilli, V., Scopa, C., Saraulli, D., Costanzi, M., Scardigli, R., Rouault, J. P., Farioli-Vecchioli, S., & Tirone, F. (2017). Physical exercise rescues defective neural stem cells and neurogenesis in the adult subventricular zone of Btg1 knockout mice. *Brain Structure and Function*, *222*, 2855–2876.

Morshead, C. M., Benveniste, P., Iscove, N. N., & van der Kooy, D. (2002). Hematopoietic competence is a rare property of neural stem cells that may depend on genetic and epigenetic alterations. *Nature Medicine*, *8*, 268–273. https://doi.org/10.1038/nm0302-268

Morshead, C. M., Reynolds, B. A., Craig, C. G., McBurney, M. W., Staines, W. A., Morassutti, D., Weiss, S., & Vanderkooy, D. (1994). Neural stem-cells in the adult mammalian forebrain - a relatively quiescent subpopulation of subependymal cells. *Neuron*, *13*, 1071–1082. https://doi.org/10.1016/0896-6273(94)90046-9

Nguyen, A., Armstrong, E. A., & Yager, J. Y. (2015). Unilateral common carotid artery ligation as a model of perinatal asphyxia: The original Rice-Vannucci model. Springer Protocols. *Neuromethods*, *104*, 1–13.

Nusrat, L., Livingston-Thomas, J. M., Raguthevan, V., Adams, K., Vonderwalde, I., Corbett, D., & Morshead, C. M. (2018). Cyclosporin A-mediated activation of endogenous neural precursor cells promotes cognitive recovery in a mouse model of stroke. *Frontiers in Aging Neuroscience*, *10*, 9. https://doi.org/10.3389/fnagi.2018.00093

Paredes, M. F., James, D., Gil-Perotin, S., Kim, H., Cotter, J. A., Ng, C., Sandoval, K., Rowitch, D. H., Xu, D., McQuillen, P. S., Garcia-Verdugo, J.-M., Huang, E. J., & Alvarez-Buylla, A. (2016). Extensive migration of young neurons into the infant human frontal lobe. *Science*, *354*, 6803. https://doi.org/10.1126/science.aaf7073

Ponti, G., Obernier, K., Guinto, C., Jose, L., Bonfanti, L., & Alvarez-Buylla, A. (2013). Cell cycle and lineage progression of neural progenitors in the ventricular-subventricular zones of adult mice. *Proceedings of the National Academy of Sciences of the USA*, *110*, E1045–E1054. https://doi.org/10.1073/pnas.1219563110

Privat, A., & Leblond, C. P. (1972). The subependymal layer and neighboring region in the brain of the young rat. *The Journal of Comparative Neurology*, *146*, 277–302.

Qu, H. L., Zhao, M., Zhao, S. S., Xiao, T., Song, C. G., Cao, Y. P., Jolkkonen, J., & Zhao, C. S. (2015). Forced limb-use enhanced neurogenesis and behavioral recovery after stroke in the aged rats. *Neuroscience*, *286*, 316–324. https://doi.org/10.1016/j.neuroscience.2014.11.040

Rha, D. W., Kang, S. W., Park, Y. G., Cho, S. R., Lee, W. T., Lee, J. E., Nam, C. M., Han, K. H., & Park, E. S. (2011). Effects of constraint-induced movement therapy on neurogenesis and functional recovery after early hypoxic-ischemic injury in mice. *Developmental Medicine and Child Neurology*, *53*, 327–333.

Ruddy, R. M., Adams, K. V., & Morshead, C. M. (2019). Age- and sex-dependent effects of metformin on neural precursor cell activation and cognitive recovery in a model of neonatal stroke. *Science Advances*, *5*(eaax1912), 1–10.

Sachewsky, N., Hunt, J., Cooke, M. J., Azimi, A., Zarin, T., Miu, C., Shoichet, M. S., & Morshead, C. M. (2014). Cyclosporin A enhances neural precursor cell survival in mice through a calcineurin-independent pathway. *Disease Models & Mechanisms*, *7*, 953–961.

Saraulli, D., Costanzi, M., Mastrorilli, V., & Farioli-Vecchioli, S. (2017). The long run: Neuroprotective effects of physical exercise on adult neurogenesis from youth to old age. *Current Neuropharmacology*, *15*, 519–533. https://doi.org/10.2174/1570159X14666160412150223

Sawaki, L., Butler, A. J., Leng, X. Y., Wassenaar, P. A., Mohammad, Y. M., Blanton, S., Sathian, K., Nichols-Larsen, D. S., Wolf, S. L., Good, D. C., & Wittenberg, G. F. (2014). Differential patterns of cortical reorganization following constraint-induced movement therapy during early and late period after stroke: A preliminary study. *NeuroRehabilitation*, *35*, 415–426. https://doi.org/10.3233/NRE-141132

Serdar, M., Kempe, K., Rizazad, M., Herz, J., Bendix, I., Felderhoff-Müser, U., & Sabir, H. (2019). Early pro-inflammatory microglia activation after inflammation-sensitized hypoxic-ischemic brain injury in neonatal rats. *Frontiers in Cellular Neuroscience*, *13*, 237. https://doi.org/10.3389/fncel.2019.00237

Smart, I. (1961). The subependymal layer of the mouse brain and its cell production as shown by radioautography after thymidine-H^3 injection. *The Journal of Comparative Neurology*, *116*, 325–347. https://doi.org/10.1002/cne.901160306

Sorrells, S. F., Paredes, M. F., Cebrian-Silla, A., Sandoval, K., Qi, D., Kelley, K. W., James, D., Mayer, S., Chang, J., Auguste, K. I., Chang, E. F., Gutierrez, A. J., Kriegstein, A. R., Mathern, G. W., Oldham, M. C., Huang, E. J., Garcia-Verdugo, J. M., Yang, Z., & Alvarez-Buylla, A. (2018). Human hippocampal neurogenesis drops sharply in children to undetectable levels in adults. *Nature*, *555*(7696), 377–381.

Taub, E. (2012). The v-analytic origins of constraint-induced movement therapy: An example of behavioral neurorehabilitation. *Behavior Analysis*, *35*, 155–178.

Taub, E., Ramey, S. L., DeLuca, S., & Echols, K. (2004). Efficacy of constraint-induced movement therapy for children with cerebral palsy with asymmetric motor impairment. *Pediatrics*, *113*, 305–312. https://doi.org/10.1542/peds.113.2.305

Taub, E., Uswatte, G., & Mark, V. W. (2014). The functional significance of cortical reorganization and the parallel development of CI therapy. *Frontiers in Human Neuroscience*, *8*, https://doi.org/10.3389/fnhum.2014.00396

Tay, T. L., Mai, D., Dautzenberg, J., Fernandez-Klett, F., Lin, G., Sagar, D. M., Drougard, A., Stempfl, T., Ardura-Fabregat, A., Staszewski, O., Margineanu, A., Sporbert, A., Steinmetz, L. M., Pospisilik, J. A., Jung, S., Priller, J., Grun, D., Ronneberger, O., & Prinz, M. (2017). A new fate mapping system reveals context-dependent random or clonal expansion of microglia. *Nature Neuroscience*, *20*, 793–803.

Ten, V. S., Bradley-Moore, M., Gingrich, J. A., Stark, R. I., & Pinsky, D. J. (2003). Brain injury and neurofunctional deficit in neonatal mice with hypoxic-ischemic encephalopathy. *Behavioural Brain Research*, *145*, 209–219.

Uswatte, G., & Taub, E. (2013). Constraint-induced movement therapy: a method for harnessing neuroplasticity to treat motor disorders. In M. M. Merzenich, M. Nahum, & T. M. VanVleet (eds) *Changing Brains*, *207*, 379–401.

Vannucci, R. C., Connor, J. R., Mauger, D. T., Palmer, C., Smith, M. B., Towfighi, J., & Vannucci, S. J. (1999). Rat model of perinatal hypoxic-ischemic brain damage. *Journal of Neuroscience Research*, *55*, 158–163.

Vay, S. U., Flitsch, L. J., Rabenstein, M., Rogall, R., Blaschke, S., Kleinhaus, J., Reinert, N., Bach, A., Fink, G. R., Schroeter, M., & Rueger, M. A. (2018). The plasticity of primary microglia and their multifaceted effects on endogenous neural stem cells in vitro and in vivo. *Journal of Neuroinflammation*, *15*, https://doi.org/10.1186/s12974-018-1261-y

Xerri, C., Zennou-Azogui, Y., Sadlaoud, K., & Sauvajon, D. (2014). Interplay between intra- and interhemispheric remodeling of neural networks as a substrate of functional recovery after stroke: Adaptive versus maladaptive reorganization. *Neuroscience*, *283*, 178–201. https://doi.org/10.1016/j.neuroscience.2014.06.066

Yamashita, T., Ninomiya, M., Acosta, P. H., Garcia-Verdugo, J. M., Sunabori, T., Sakaguchi, M., Adachi, K., Kojima, T., Hirota, Y., Kawase, T., Araki, N., Abe, K., Okano, H., & Sawamoto, K. (2006). Subventricular zone-derived neuroblasts migrate and differentiate into mature neurons in the post-stroke adult striatum. *Journal of Neuroscience*, *26*, 6627–6636.

Yang, Z., Covey, M. V., Bitel, C. L., Ni, L., Jonakait, G. M., & Levison, S. W. (2007). Sustained neocortical neurogenesis after neonatal hypoxic/ischemic injury. *Annals of Neurology*, *61*, 199–208.

Yang, Z., & Levison, S. W. (2006). Hypoxia/ischemia expands the regenerative capacity of progenitors in the perinatal subventricular zone. *Neuroscience*, *139*, 555–564. https://doi.org/10.1016/j.neuroscience.2005.12.059

Zhang, R. L., Zhang, Z. G., Zhang, L., & Chopp, M. (2001). Proliferation and differentiation of progenitor cells in the cortex and the subventricular zone in the adult rat after focal cerebral ischemia. *Neuroscience*, *105*, 33–41. https://doi.org/10.1016/S0306-4522(01)00117-8

Zhao, C. S., Wang, J., Zhao, S. S., & Nie, Y. X. (2009). Constraint-induced movement therapy enhanced neurogenesis and behavioral recovery after stroke in adult rats. *Tohoku Journal of Experimental Medicine*, *218*, 301–308.

Zhao, S. S., Zhao, M., Xiao, T., Jolkkonen, J., & Zhao, C. S. (2013). Constraint-induced movement therapy overcomes the intrinsic axonal growth-inhibitory signals in stroke rats. *Stroke*, *44*, 1698–1705. https://doi.org/10.1161/STROKEAHA.111.000361

Zhao, S. S., Zhao, Y., Xiao, T., Zhao, M., Jolkkonen, J., & Zhao, C. S. (2013). increased neurogenesis contributes to the promoted behavioral recovery by constraint-induced movement therapy after stroke in adult rats. *CNS Neuroscience & Therapeutics*, *19*, 194–196. https://doi.org/10.1111/cns.12058

SUPPORTING INFORMATION

Additional supporting information may be found online in the Supporting Information section.

How to cite this article: Adams KV, Mahmud N, Green-Holland M, et al. Constraint-induced movement therapy promotes motor recovery after neonatal stroke in the absence of neural precursor activation. *Eur J Neurosci*. 2021;53:1334–1349. https://doi.org/10.1111/ejn.14993